Jpn. J. Cancer Res. **93**, 284–290, March 2002

Multiplexed Analysis of Post-PCR Fluorescence-labeled Microsatellite Alleles and Statistical Evaluation of Their Imbalance in Brain Tumors

Koji Yoshimoto,[1] Toru Iwaki,[2] Takanori Inamura,[3] Masashi Fukui,[3] Tomoko Tahira[1] and Kenshi Hayashi[1, 4]

[1]Division of Genome Analysis, Research Center for Genetic Information, Medical Institute of Bioregulation, [2]Department of Neuropathology and [3]Department of Neurosurgery, Graduate School of Medical Sciences, Kyushu University, 3-1-1 Maidashi, Higashi-ku, Fukuoka 812-8582

Detection of the loss of chromosomal regions in cancerous tissues has diagnostic and prognostic relevance, and the development of a reliable and cost-effective technique for this is clinically important. Here we present an efficient technique for quantitative detection of microsatellite alleles, using a post-PCR fluorescence-labeling procedure and multiplexed analysis. We also present a new statistical method for the interpretation of the data that permits reliable and sensitive evaluation of the allelic status of sampled DNA. A high-resolution analysis of allelic imbalance on chromosomes 1p, 10 and 19q in 28 glioma samples of various types using this method revealed that allelic imbalances are more frequent than have been reported, suggesting the diagnostic value of this method in examining the genetic profiles of gliomas.

Key words: Glioma — Chromosome 10 — Statistical assessment — Allelic imbalance — Post-PCR fluorescence-labeling

Loss of heterozygosity (LOH), is frequently observed as a genetic alteration in various kinds of cancer tissues, and is considered to be a genetic mechanism that leads to inactivation of tumor suppressor genes. The region of LOH, often detected as an allelic imbalance, is different between the subtypes of some tumors such as gliomas, so defining the chromosomal regions that reveal allelic imbalance can have a diagnostic value. For example, in gliomas, loss of chromosome regions on 1p and 19 is frequent in oligodendrogliomas, and deletions on chromosome 10 may be associated with high-grade astrocytic gliomas.[1–3] However, it is still uncertain if these genetic changes can serve as diagnostic indicators, since the percentage of these changes varies between reports,[4] and the techniques used to detect the imbalance are costly.

Multiplexed fluorescence-based quantitative evaluation of microsatellite alleles using DNA sequencers is frequently used for the detection of allelic imbalance. However, this method usually requires numerous fluorescently labeled primers, which are expensive. In addition, the sets of markers in the multiplex analysis using pre-labeled primers are inflexible. To change the combination of the markers or to include new markers in the multiplexing, considerable investment is often needed for the synthesis or purchase of new primers. Using allele quantification of microsatellites also often leads to contradictory determinations of imbalance, because of unsettled criteria for interpretation of the data.[4] Assessment of allelic imbalance is difficult because of the heterogeneity of tumor cells and the presence of normal cells in tumor biopsies. Thus, perfect allelic imbalance — absolute lack of one allele — can never be observed in surgical specimens without extra study, such as microdissection or culturing to obtain clonal tumor cell populations. However, those steps require special expertise, and are diagnostically impractical.

Allelic imbalances are usually detected, based on the comparison of the peak height ratio of two alleles in tumor and normal tissues of heterozygous individuals, after electrophoretic separation of alleles in PCR-amplified products. In many published reports, tumors have been scored as having LOH if the relative fluorescence ratios of the two alleles in the tumor sample differ by more than 1.5–2.0-fold compared with that of normal tissue. However, these cut-off values have been arbitrary. This ambiguity of the criteria for judgment of imbalance is at least a part of the reason for the discrepancies in the reported percentages of values of allelic imbalance.

The aim of this study was to develop a practical method to assess the allelic status of tumor cells. Post-PCR fluorescence-labeling procedures were employed instead of using pre-labeled fluorescent primers, and this allowed us to assess the allelic status of many microsatellite markers at a low cost using widely available DNA sequencers.[5] Another advantage of post-labeling procedures is that the combination of markers in each multiplexed electrophoresis is flexible. We also established objective criteria for the detection of allelic imbalance based on statistical interpretation of the data, which permitted sensitive and reliable detection of the chromosomal regions of allelic imbalance. Using these criteria, we evaluated the allelic status of chromosomes 1p, 10 and 19q, and tumor suppressor genes

[4] To whom correspondence should be addressed.
E-mail: khayashi@gen.kyushu-u.ac.jp

p53 and *CDKN2A* (*p16*) in 28 gliomas. We found that the characteristic allelic imbalance in the subtypes of the tumor, in particular the loss of chromosome 10 in astrocytomas, is higher than previously reported, and can be a useful diagnostic indicator.

MATERIALS AND METHODS

Tumor and control samples Samples of brain tumors were obtained from patients during craniotomy at Kyushu University Hospital or other affiliated institutions. Part of the tumor tissues was saved for histopathological examination, and the rest was snap-frozen in liquid nitrogen and stored at −80°C. Tumors were histologically diagnosed by a neuropathologist and graded according to WHO criteria.[6] The samples consisted of 18 astrocytic high-grade gliomas, eight oligodendrogliomas and two mixed oligoastrocytomas. The astrocytic gliomas included three grade III anaplastic astrocytomas and 15 grade IV glioblastomas. Oligodendrogliomas included seven grade II oligodendrogliomas and one grade III anaplastic oligodendroglioma. Mixed oligoastrocytomas included one grade II oligoastrocytoma and one grade III anaplastic oligoastrocytoma. Tumor DNA was isolated from the frozen blocks using standard phenol-chloroform extraction procedures. Corresponding normal DNA was isolated from a blood sample of the same patient. Use of all materials in this study was in accordance with the guidelines of the Ethics Committee of Kyushu University.

Microsatellite markers The 78 sequence tagged sites carrying dinucleotide repeats on chromosomes 1p, 10 and 19q were chosen from the list of HD5 ABI PRISM Linkage Mapping Set (Applied Biosystems, Foster City, CA). We also examined markers D10S216, D19S219, D19S412 and D19S596, as these have been frequently used in studies of LOH in these chromosomal regions.[7–10] Loci of the known tumor suppressor genes *p53* and *CDKN2A* (*p16*) were examined using markers on chromosomes 17p (D17S831, D17S1876, and D17S1791) and 9p (D9S269, D9S156, D9S157, and D9S171), respectively. The primer sequences of all markers were obtained from the Genome Database (http://www.gdb.org/). The order of microsatellite markers on the chromosomes was according to relevant data on the Web sites at Ensemble (http://ensembl.org/) and at Human Genome Working Draft (http://genome.ucsc.edu/). All primer sequences were modified to contain either ATT (forward primer) or GTT (reverse primer) at their 5′ ends for post-PCR fluorescence-labeling purposes,[11] and were purchased as desalted reagents (Amersham Pharmacia Biotech, Tokyo). Primer sequences are available on request.

Polymerase chain reaction PCR was performed in a total volume of 5 μl containing 30–50 ng of template DNA, 1 μM of each primer, 0.2 m*M* of each nucleotide, 0.125 U of *Taq* DNA polymerase (Applied Biosystems), 27.5 ng of *Taq*-Start antibody (Clontech Laboratories, Palo Alto, CA), 2.5 m*M* $MgCl_2$, 10 m*M* Tris-HCl, pH 8.3, and 50 m*M* KCl. PCR was performed in a thermal cycler (Biometra, Goettingen, Germany) with an initial denaturation step at 95°C for 1 min, followed by 35 cycles of 30 s at 95°C, 30 s at 65°C, and 1 min at 72°C. Final extension was for 5 min at 72°C. An annealing temperature of 60°C was adopted for markers D9S156 and D9S269. PCR reactions on tumor DNA and the corresponding blood DNA were performed in the same batch.

Pooling of markers and fluorescence-labeling for multiplexed analysis The combination of markers in each multiplexed analysis was determined as follows. The PCR amplicons to be multiplexed were divided into two to four size classes, each containing three amplicons. The amplicons, one per size class, were then pooled (2 μl per amplicon). In this way, three pools, each containing two to four amplicons that did not overlap in size, were obtained. The pools were then subjected to post-labeling reactions using different fluorophores for the three pools: R6G-dCTP, R110-dUTP and TAMRA-dUTP (Applied Biosystems). The reaction was started by adding an equal volume of 5 m*M* Tris-HCl pH 8.7, 10 m*M* $MgCl_2$, 0.1 U/μl Klenow fragment DNA polymerase I, and either 2 μM R6G-dCTP, R110-dUTP or TAMRA-dUTP. In this reaction, the strand having corresponding nucleotides at the 3′ end was fluorescently labeled, while the other strand remained unlabeled. The products labeled with the three different fluorophores were then combined, a 6-carboxy-X-rhodamine (ROX)-labeled size marker (GS400HD [ROX]; Applied Biosystems, 0.5 μl) was added, and the mixture was subjected to capillary electrophoresis after 15-fold dilution with distilled water.

Electrophoresis and data processing Capillary electrophoresis was performed with a 310 Prism Genetic Analyzer (Applied Biosystems). Raw electrophoresis data were analyzed with "GeneScan" Analysis software (Applied Biosystems) as described previously.[5] Alleles were identified, and peak heights were measured using "Genotyper" software (Applied Biosystems).

RESULTS

Effectiveness of the post-PCR fluorescence-labeling method We adopted a post-PCR fluorescence labeling method to label and quantify microsatellite alleles in the DNA of tumor and blood samples. In the method described here, the designing of multiplexed analysis is straightforward, because each microsatellite marker can be labeled with any of the three fluorophores. Moreover, allele peaks in the electropherogram of post-labeled products are free from non-templated plus-A peaks, because the Klenow fragment of DNA polymerase I used in the

labeling reaction effectively removes the extra nucleotide. As a result, resolution of the peaks is improved and alleles can be identified reliably, and, as shown in Fig. 1, most of the microsatellite ladders are separated to the baseline. In the example of LOH analysis shown in this figure, six microsatellite markers on chromosome 1p in a glioblastoma and in normal cells derived from the same individual were analyzed, and the imbalance is clearly seen for all markers.

Reproducibility of peak height ratio of alleles in normal samples In PCR-based microsatellite analysis, interpretation of electropherograms of heterozygous individuals is often complicated by the presence of stutters, especially when the difference between the repeat units of alleles is small. We have developed a simple quantitative method to statistically evaluate allelic status without the often laborious and unreliable procedures of stutter-correction.

We defined R_N as the ratio of the height of the major peak of the smaller allele to that of the larger allele in the normal tissue (blood) of heterozygous individuals, without correction of the stutter effect. Similarly, R_T was defined for the ratio in the tumor sample. Allelic status was then assessed from the absolute value of difference (ΔR) between R_N and R_T. That is, the tumor is in a state of allelic imbalance when R_T is significantly different from R_N.

To estimate the variability of R_N, we took 550 heterozygous cases (82 loci in 28 individuals), and the standard deviations of R_N (σR_N) for all cases were calculated using five independent determinations for each case (a total of 2750 PCR amplifications). We found that the R_N widely varied if the products of different PCR batches were compared. However, the variations of R_N obtained within the same PCR batch (intra-PCR variation) were moderately small. We therefore decided to consider intra-PCR variations, and estimated their standard deviations. We then plotted σR_N against the mean value of R_N. The results revealed that σR_N can be approximated by a regression line, although considerable scatter of the plots was observed (Fig. 2), and the following relationship is established:

$$\sigma R_N = 0.05 \times \overline{R_N}$$

Here, the slope, 0.05, is the coefficient of variation of R_N.

Statistical assessment of allelic status To determine whether R_T, the ratio of peak heights of alleles in the tumor, is significantly different from R_N (the ratio in the

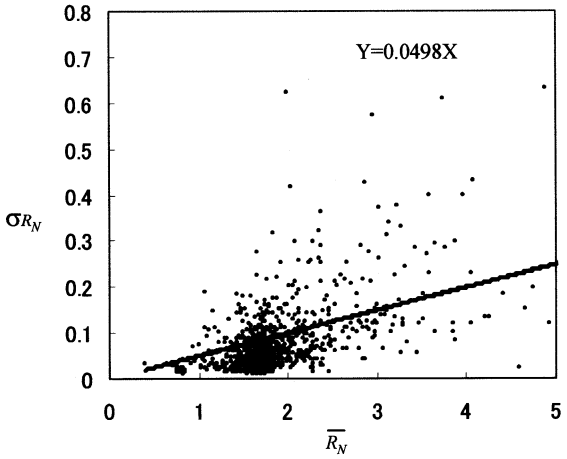

Fig. 2. The relationship between the standard deviation of R_N (σR_N) and the mean value of R_N ($\overline{R_N}$). σR_N for 550 heterozygous cases (82 loci) was calculated by five successive determinations for all cases, and plotted against $\overline{R_N}$. The solid line shows the linear regression line, which was used to estimate the variability of R_N.

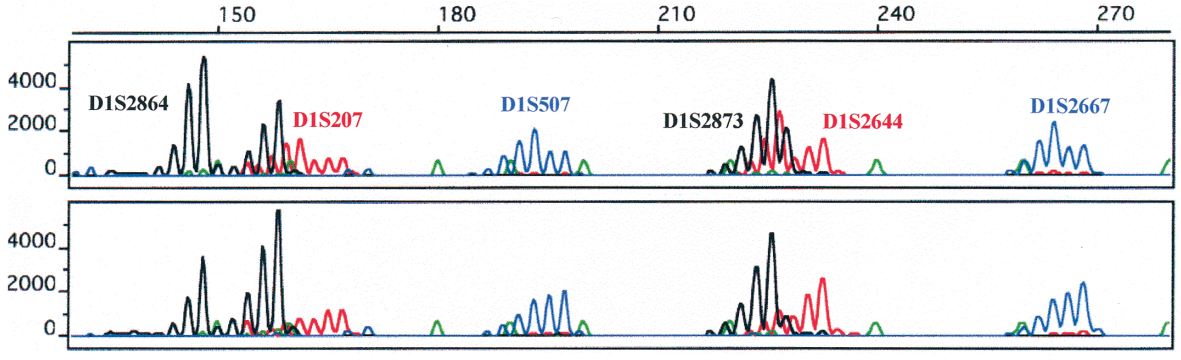

Fig. 1. Representative electropherograms of multiplex microsatellite analysis for LOH assessment. Electropherograms of normal samples (top) and of tumor samples (bottom) in the same patient (GB9) are shown. The ordinate represents the fluorescence intensity of the peaks in arbitrary units. The size in nucleotides is shown at the top of the figure. Names of the markers are shown above the allele peaks. The peaks colored in red, blue and black represent samples labeled with R6G-dCTP, R110-dUTP and TAMRA-dUTP, respectively, by the post-PCR fluorescent-labeling technique. Peaks in green are those of ROX-labeled size markers.

normal tissue), a tolerance range of R_N is estimated at a confidence of $1-\alpha$ from Student's t test, that is,

$$R_N \pm t_{n-1}\left(\frac{\alpha}{2}\right) \times \sigma_{R_N} \sqrt{\frac{n+1}{n}}$$

where n is the number of analyzed samples.[12] Here, σ_{R_N} was estimated from five determinations of normal samples, thus $n=5$. From the equation above, an R_T value outside $R_N \pm 6\sigma_{R_N}$ is considered to be significantly different from R_N with more than 99% confidence, i.e., there is a false-positive rate of less than 1% using this criterion of allelic imbalance.

Using these approach, we examined the allelic status of all tumors using the 89 markers, which involved 2492 genotypings, and defined the allelic imbalances. Fig. 3 shows the distribution of ΔR within bins of width σ_{R_N}. The distribution of ΔR was found to be bimodal, and the smallest value was observed between $5\sigma_{R_N}$ and $6\sigma_{R_N}$, justifying our definition of the cut-off limit for allelic balance as $6\sigma_{R_N}$, with a low false-negative rate.

Allelic status of gliomas Having established objective criteria for the judgment of allelic imbalance, we assessed the allelic status of candidate chromosomes in gliomas. As shown in Fig. 4, the pattern of allelic imbalance in our results agrees with previously reported genetic alterations characteristic of oligodendroglioma and astrocytic gliomas. However, the frequencies are higher than those that have been previously reported. For example, concomitant losses of entire chromosomes 1p and 19q were observed in 90% of oligodendrogliomas in this study, in contrast to 50–80% in previous reports.[2, 3, 13, 14] Allelic imbalances of 1p and 19q in astrocytic gliomas were also 39% and 61%, respectively, whereas the highest reported frequencies are 20% and 40%.[10, 14–17] In addition, the frequency of allelic imbalance on chromosome 10 is 94%, a value higher than that in many previous reports,[7, 8, 18–20] while none was observed in oligodendrogliomas. As shown in Fig. 5, allelic imbalance of the *p53* and *CDKN2A* (*p16*) loci was detected in both oligodendroglial tumors and astrocytic gliomas.

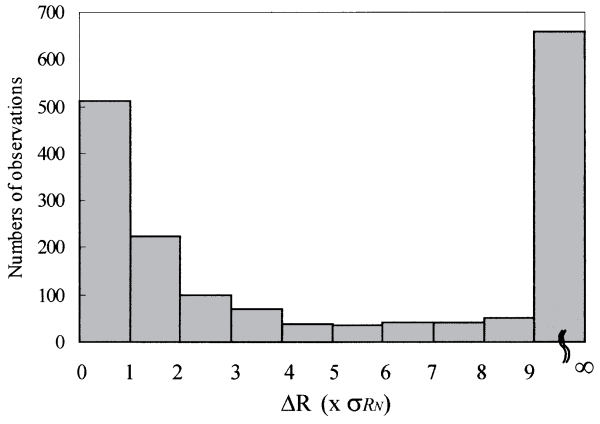

Fig. 3. Distributions of the absolute value of difference (ΔR) between R_N and R_T of 928 informative genotypes within the bins of width σ_{R_N}. Note that the numbers of observations are minimum when ΔR is between $5\sigma_{R_N}$ and $6\sigma_{R_N}$.

Microsatellite instability In the process of assessing LOH, we identified several loci with microsatellite instability, which were evaluated according to the criteria reported by Sobrido *et al.*[21] As shown in Fig. 4, microsatellite instability was observed in 12 of the 2492 examined loci (0.4%).

DISCUSSION

LOH is frequently detected in many common cancers, but the tumor suppressor genes or their loci responsible for the cancer have not necessarily been identified. Therefore, the search for allelic imbalance for the detection of LOH requires an analysis involving many markers located at a high density.

The multiplexed analysis of post-PCR fluorescence-labeled microsatellite markers employed here is cost-effective, because the procedure does not require the synthesis of expensive fluorescently pre-labeled primers. Besides, each microsatellite marker can be labeled with any fluorescent dye; thus, multiplexed analysis is easily designed using combinations of products labeled with desired fluorophores. In the initial design of the multiplexing we found that the peak of one marker product overlapped with the neighboring marker labeled with the same fluorophore, causing problems in the identification of the alleles. The problem was solved by replacing the fluorophore of one of the overlapping markers with that of another in the same size range.

In many previous reports, the allelic imbalance factor (AIF), defined as the value of R_T/R_N, has been employed as an indicator to detect the imbalance in fluorescence-based microsatellite allele quantification. However, several cut-off values have been arbitrarily used among the reports. For example, Canzian *et al.*[22] defined 1.67 as a cut-off value, whereas other reports adopted different values, such as 1.5[23] or 2.0.[24] The inconsistency in the reported occurrence of imbalance may thus be attributable to the ambiguity of the definition of the cut-off value.

In the assessment of variability of R_N, Wang *et al.*[25] and Hampton *et al.*[26] have reported that R_N can fluctuate by 20%, and they defined a tumor as having LOH when the ratio (R_T) is found outside this range. However, the numbers of normal samples used for evaluating the variability in their studies were small, and the studies did not take into account the variability of R_N, which differs according to its value.

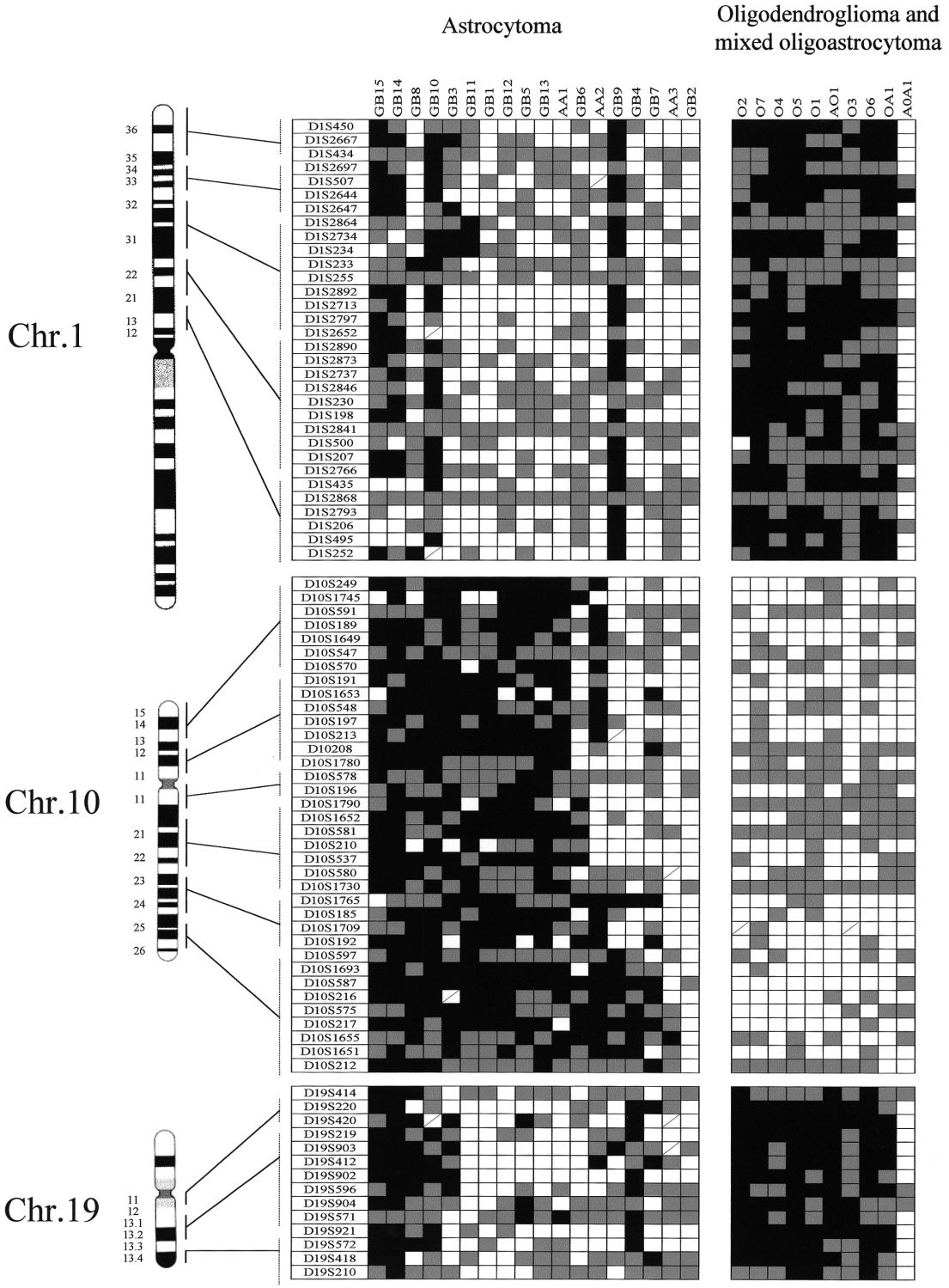

Fig. 4. High-resolution allelotyping of chromosomes 1p, 10 and 19q. Complete allelotyping results of 18 high-grade astrocytomas, eight oligodendrogliomas and two mixed oligoastrocytomas. Microsatellite markers are shown on the left. Case numbers are indicated at the top. AA, anaplastic astrocytoma; GB, glioblastoma; O, oligodendroglioma; AO, anaplastic oligodendroglioma; OA, oligoastrocytoma; AOA, anaplastic oligoastrocytoma. Black box, allelic imbalance; white box, heterozygous; gray box, marker tested but not informative (homozygous in the normal DNA); box with slash, microsatellite instability.

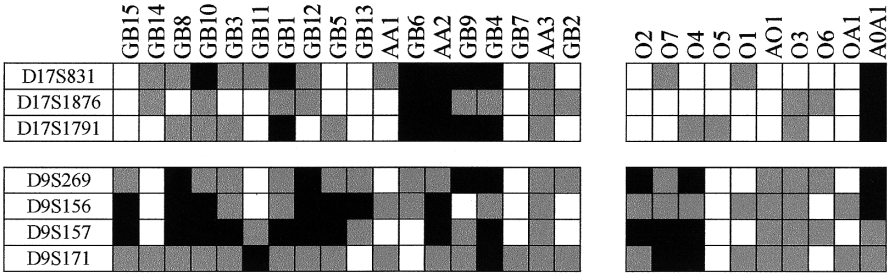

Fig. 5. Allelotyping of p53 and CDKN2A loci. The order of case numbers is the same as in Fig. 4. □ retention, ▨ not informative, ■ allelic imbalance.

In the assessment of microsatellite alleles proposed here, we judged the tumor to have allelic imbalance when the peak height ratio of alleles was statistically significantly different from that of normal. As shown in Fig. 2, we found that the standard deviation of R_N (σR_N) varies, and is roughly proportional to R_N. This relationship was used to estimate the σR_N of each genotype. We then set the cut-off value at six times σR_N. At this setting, the possibility of false positives in the judgment of allelic loss is less than 1%, assuming that the ratio follows Student's *t* distribution. The false negative rate is expected to be low, as demonstrated in Fig. 3, although its exact percentage is unknown. Also, as has been described previously,[27] the relative peak height of alleles using post-PCR fluorescence-labeling can be quantified within an error range of 1.8%. This is small enough for the detection of allelic imbalance when PCR products of the same batch are compared.

We compared the sensitivity of the two methods, the AIF method and ours, using the same samples. The cut-off value was set to 1.5, the most sensitive criterion among the previous reports, and the imbalances were scored for all the markers on chromosome 10. We found that out of the 300 loci detected as imbalanced in our method, 62 (20%) failed to be detected in the AIF method (data not shown). None of the loci constitutively heterozygous in our method was judged to be at imbalance in the AIF method. Thus, our method is clearly more sensitive. The specific patterns of the imbalance detected by our method, i.e., contiguity of most of the loci of imbalance found, strongly argue that our approach is valid.

From the biological standpoint, allelic imbalances of chromosomes 1p and 19q are observed in both of the histologically different gliomas, although the frequencies are somewhat different. On the other hand, loss of chromosome 10 seems to be the most discriminative genetic alteration that distinguishes astrocytic gliomas from oligodendrogliomas, an observation that confirms some previous reports and opens the possibility that this chromosomal aberration may be useful as a clinical indicator of astrocytic gliomas.

ACKNOWLEDGMENTS

We thank Ms. Naoka Fujie for her technical assistance. This study was supported by a Grant-in-Aid for "Genome Science" from the Ministry of Education, Culture, Sports, Science and Technology, Japan.

(Received November 26, 2001/Accepted December 20, 2001)

REFERENCES

1) Louis, D. N. and Gusella, J. F. A tiger behind many doors: multiple genetic pathways to malignant glioma. *Trends Genet.*, **11**, 412–415 (1995).
2) Rasheed, B. K., Wiltshire, R. N., Bigner, S. H. and Bigner, D. D. Molecular pathogenesis of malignant gliomas. *Curr. Opin. Oncol.*, **11**, 162–167 (1999).
3) Maher, E. A., Furnari, F. B., Bachoo, R. M., Rowitch, D. H., Louis, D. N., Cavenee, W. K. and DePinho, R. A. Malignant glioma: genetics and biology of a grave matter. *Genes Dev.*, **15**, 1311–1333 (2001).
4) Devilee, P., Cleton-Jansen, A. and Cornelisse, C. J. Ever since Knudson. *Trends Genet.*, **17**, 569–573 (2001).
5) Kondo, H., Tahira, T., Hayashi, H., Oshima, K. and Hayashi, K. Microsatellite genotyping of post-PCR fluorescently labeled markers. *Biotechniques*, **29**, 868–872 (2000).
6) Kleihues, P., Burger, P. C. and Scheithauer, B. W. "Histological Typing of Tumors of the Central Nervous System. World Health Organization International Histological Classification of Tumors," 2nd Ed. (1993). Springer Verlag, Berlin.
7) Albarosa, R., Colombo, B. M., Roz, L., Magnani, I., Pollo, B., Cirenei, N., Giani, C., Conti, A. M., DiDonato, S. and Finocchiaro, G. Deletion mapping of gliomas suggests the

presence of two small regions for candidate tumor-suppressor genes in a 17-cM interval on chromosome 10q. *Am. J. Hum. Genet.*, **58**, 1260–1267 (1996).
8) Fujisawa, H., Reis, R. M., Nakamura, M., Colella, S., Yonekawa, Y., Kleihues, P. and Ohgaki, H. Loss of heterozygosity on chromosome 10 is more extensive in primary (*de novo*) than in secondary glioblastomas. *Lab. Invest.*, **80**, 65–72 (2000).
9) Cairncross, J. G., Ueki, K., Zlatescu, M. C., Lisle, D. K., Finkelstein, D. M., Hammond, R. R., Silver, J. S., Stark, P. C., Macdonald, D. R., Ino, Y., Ramsay, D. A. and Louis, D. N. Specific genetic predictors of chemotherapeutic response and survival in patients with anaplastic oligodendrogliomas. *J. Natl. Cancer Inst.*, **90**, 1473–1479 (1998).
10) Nakamura, M., Yang, F., Fujisawa, H., Yonekawa, Y., Kleihues, P. and Ohgaki, H. Loss of heterozygosity on chromosome 19 in secondary glioblastomas. *J. Neuropathol. Exp. Neurol.*, **59**, 539–543 (2000).
11) Inazuka, M., Tahira, T. and Hayashi, K. One-tube post-PCR fluorescent labeling of DNA fragments. *Genome Res.*, **6**, 551–557 (1996).
12) Ross, S. M. "Introduction to Probability and Statistics for Engineers and Scientists," 2nd Ed., pp. 293 (2000). Harcourt Academic Press, San Diego.
13) Zhu, J. J., Santarius, T., Wu, X., Tsong, J., Guha, A., Wu, J. K., Hudson, T. J. and Black, P. M. Screening for loss of heterozygosity and microsatellite instability in oligodendrogliomas. *Genes Chromosom. Cancer*, **21**, 207–216 (1998).
14) Smith, J. S., Alderete, B., Minn, Y., Borell, T. J., Perry, A., Mohapatra, G., Hosek, S. M., Kimmel, D., O'Fallon, J., Yates, A., Feuerstein, B. G., Burger, P. C., Scheithauer, B. W. and Jenkins, R. B. Localization of common deletion regions on 1p and 19q in human gliomas and their association with histological subtype. *Oncogene*, **18**, 4144–4152 (1999).
15) von Deimling, A., Bender, B., Jahnke, R., Waha, A., Kraus, J., Albrecht, S., Wellenreuther, R., Fassbender, F., Nagel, J. and Menon, A. G. Loci associated with malignant progression in astrocytomas: a candidate on chromosome 19q. *Cancer Res.*, **54**, 1397–1401 (1994).
16) von Deimling, A., Nagel, J., Bender, B., Lenartz, D., Schramm, J., Louis, D. N. and Wiestler, O. D. Deletion mapping of chromosome 19 in human gliomas. *Int. J. Cancer*, **57**, 676–680 (1994).
17) Smith, J. S., Perry, A., Borell, T. J., Lee, H. K., O'Fallon, J., Hosek, S. M., Kimmel, D., Yates, A., Burger, P. C., Scheithauer, B. W. and Jenkins, R. B. Alterations of chromosome arms 1p and 19q as predictors of survival in oligodendrogliomas, astrocytomas and mixed oligoastrocytomas. *J. Clin. Oncol.*, **18**, 636–645 (2000).
18) Lang, F. F., Miller, D. C., Koslow, M. and Newcomb, E. W. Pathways leading to glioblastoma multiforme: a molecular analysis of genetic alterations in 65 astrocytic tumors. *J. Neurosurg.*, **81**, 427–436 (1994).
19) Sonoda, Y., Murakami, Y., Tominaga, T., Kayama, T., Yoshimoto, T. and Sekiya, T. Deletion mapping of chromosome 10 in human glioma. *Jpn. J. Cancer Res.*, **87**, 363–367 (1996).
20) Ichimura, K., Schmidt, E. E., Miyakawa, A., Goike, H. M. and Collins, V. P. Distinct patterns of deletion on 10p and 10q suggest involvement of multiple tumor suppressor genes in the development of astrocytic gliomas of different malignancy grades. *Genes Chromosom. Cancer*, **22**, 9–15 (1998).
21) Sobrido, M. J., Pereira, C. R., Barros, F., Forteza, J., Carracedo, A. and Lema, M. Low frequency of replication errors in primary nervous system tumours. *J. Neurol. Neurosurg. Psychiatry*, **69**, 369–375 (2000).
22) Canzian, F., Salovaara, R., Hemminki, A., Kristo, P., Chadwick, R. B., Aaltonen, L. A. and de la Chapelle, A. Semiautomated assessment of loss of heterozygosity and replication error in tumors. *Cancer Res.*, **56**, 3331–3337 (1996).
23) Cawkwell, L., Bell, S. M., Lewis, F. A., Dixon, M. F., Taylor, G. R. and Quirke, P. Rapid detection of allele loss in colorectal tumours using microsatellites and fluorescent DNA technology. *Br. J. Cancer*, **67**, 1262–1267 (1993).
24) Achille, A., Biasi, M. O., Zamboni, G., Bogina, G., Magalini, A. R., Pederzoli, P., Perucho, M. and Scarpa, A. Chromosome 7q allelic losses in pancreatic carcinoma. *Cancer Res.*, **56**, 3808–3813 (1996).
25) Wang, Y., Hung, S. C., Linn, J. F., Steiner, G., Glazer, A. N., Sidransky, D. and Mathies, R. A. Microsatellite-based cancer detection using capillary array electrophoresis and energy-transfer fluorescent primers. *Electrophoresis*, **18**, 1742–1749 (1997).
26) Hampton, G. M., Larson, A. A., Baergen, R. N., Sommers, R. L., Kern, S. and Cavenee, W. K. Simultaneous assessment of loss of heterozygosity at multiple microsatellite loci using semi-automated fluorescence-based detection: subregional mapping of chromosome 4 in cervical carcinoma. *Proc. Natl. Acad. Sci. USA*, **93**, 6704–6709 (1996).
27) Sasaki, T., Tahira, T., Suzuki, A., Higasa, K., Kukita, Y., Baba, S. and Hayashi, K. Precise estimation of allele frequencies of single-nucleotide polymorphisms by a quantitative SSCP analysis of pooled DNA. *Am. J. Hum. Genet.*, **68**, 214–218 (2001).